ACS OMEGA

http://pubs.acs.org/journal/acsodf

Article

# Solar Salt with Carbon Nanotubes as a Potential Phase Change Material for High-Temperature Applications: Investigations on Thermal Properties and Chemical Stability

Pethurajan Vigneshwaran, Saboor Shaik,* Sivan Suresh, Mohamed Abbas, Chanduveetil Ahamed Saleel, and Erdem Cuce

Cite This: *ACS Omega* 2023, 8, 17563−17572

Read Online

ACCESS | Metrics & More | Article Recommendations



**ABSTRACT:** Nano-enhanced phase change materials are highly employed for an enhanced heat-transfer process. The current work reports that the thermal properties of solar salt-based phase change materials were enhanced with carbon nanotubes (CNTs). Solar salt (60:40 of $NaNO_3/KNO_3$) with a phase change temperature and enthalpy of 225.13 °C and 244.76 kJ/kg, respectively, is proposed as a high-temperature PCM, and CNT is added to improve its thermal conductivity. The ball-milling method was employed to mix CNTs with solar salt at various concentrations of 0.1, 0.3, and 0.5% by weight. SEM images display the even distribution of CNTs with solar salt, with the absence of cluster formations. The thermal conductivity, phase change properties, and thermal and chemical stabilities of the composites were studied before and after 300 thermal cycles. FTIR studies indicated only physical interaction between PCM and CNTs. The thermal conductivity was enhanced with an increase in CNT concentration. The thermal conductivity was enhanced by 127.19 and 125.09% before and after cycling, respectively, in the presence of 0.5% CNT. The phase change temperature decreased by around 1.64% after adding 0.5% CNT, with a decrease of 14.67% in the latent heat during melting. TGA thermograms indicated the weight loss was initiated at about 590 and 575 °C before and after thermal cycling, after which it was rapid with an increase in temperature. Thermal characterization of CNT-enhanced solar salt indicated that the composites could be used as phase change materials for enhanced heat-transfer applications.

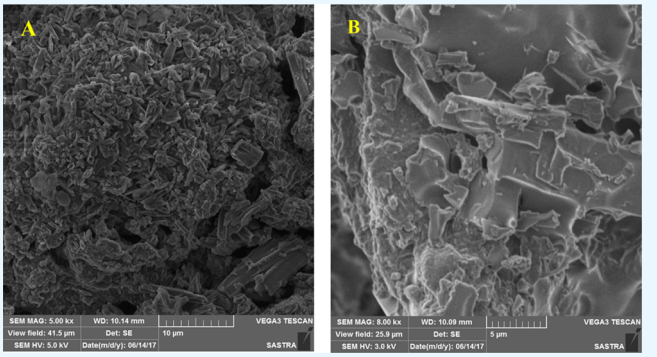


## 1. INTRODUCTION

Solar energy, an ideal heat source with countless advantages and solar energy utilization, is an efficient way to significantly reduce the energy requirement and problems caused by the usage of fossil fuels. The solar-based thermal renewable energy source can reduce the dependence on fossil fuels.[1] Thermal energy can be stored through sensible heat storage (SHS) (specific heat is utilized in storing heat),[2] chemical heat storage (CHS) (heat is stored and released based on chemical reactions and possesses high stability and energy storage density),[3] and latent heat storage (LHS) (energy is stored in the form of latent heat and has the advantage of a high energy storage density).[4] LHS-based thermal energy storage (TES) systems find application in hot water for domestic buildings,[5] utilization of solar energy,[6] and waste heat recovery.[7] Phase change materials (PCMs) are employed as heat storage media in TES systems with the advantages of a high energy storage density, constant temperature operation, low price, and a wider range of temperature availability.[8,9] PCMs are classified mostly by the melting point and thermal conductivity with respect to the application. Overall, PCMs are categorized into organic, inorganic, and eutectic materials. Paraffin and nonparaffin compounds come under the category of organic PCMs.[10] Salts, salt hydrates, and metal alloys come under inorganic PCMs.[11] In the literature, significant attention has been focused on low- and medium-temperature PCMs with fewer studies on high-temperature PCMs.[12] Certain measures need to be taken to augment the heat-transfer rate of PCMs and increase their thermal conductivity. Recently, the accumulation of highly conducting nanomaterials has been proved to improve the thermal conductivity of PCMs.[13] The addition of nanomaterials such as carbon nanotubes (CNTs) or metal or metal oxide nanoparticles augments the thermal conductivity as they possess a low density and enormous surface area.[14] CNTs

Received: November 26, 2022
Accepted: April 20, 2023
Published: May 8, 2023

possess high thermal conductivity (2000−6000 W/mK) and are dispersed in PCMs. Van der Waals attraction between the narrowed molecules and the constraining wall of CNTs holds the PCM molecules.[15] Recently, carbon-based allotropes have received major attention, increasing their usage. CNTs are lightweight materials with small particle sizes and large surface areas, which improve the molecular captivity of PCMs.[16] Recently, single-walled CNTs (SWCNTs) and multi-walled CNTs (MWCNTs) were added to hexadecyl acrylate (HDA) PCMs as thermal conductive fillers[17] through an innovative method using solvent-free Diels−Alder (DA) reaction, which showed enhancements of 134 and 339%, respectively, for SWCNTs and MWCNTs as compared to HDA. MWCNTs were dispersed in palmitic acid (PA) through mechanochemical reaction treatment along with ball-milling of a mixture of potassium hydroxide and pristine CNTs,[18] and it is reported that 0.01% CNT enhanced thermal conductivity by 46 and 38% at 25 and 65 °C, respectively, compared to PA. Various CNT concentrations were added to paraffin for cold storage,[19] and after adding 3% CNT, the thermal conductivity was reported to be enhanced by 30.3 and 28.5%, respectively, in the solid and liquid phases with corresponding enthalpy drops of 9.3 and 8.9%. Graphene and MWCNTs were mixed at various ratios with paraffin for the thermal management of lithium-ion batteries,[20] and it was reported that with a mass ratio of 3:7 of MWCNT/graphene, the thermal conductivity was enhanced by 31.8, 55.4, and 124%. Various mass fractions of MWCNTs were added to poly(ethylene glycol) 8000 (PEG8000) to investigate their thermal properties,[21] and a gradual enhancement in the thermal conductivity from 0.295 to 0.531 W/mK by adding 0.5 to 5 wt % MWCNT was reported. A series of eutectic mixtures of palmitic acid−stearic acid was prepared with mass fractions of CNTs ranging from 5 to 8 wt %,[22] and thermal conductivity enhancements of 20.2, 26.2, 26.2, and 29.7% were reported for 5, 6, 7, and 8% CNTs, respectively, along with high thermal reliability. Shile Shen et al.[23] studied the influence of modified CNTs with erythritol. They reported an augmentation in thermal conductivity from 0.19 to 0.98 W/mK in the presence of 1% MWCNTs. The nanoparticles were found to have a negligible effect on the phase transition temperatures and their corresponding enthalpies and greatly improved the thermal conductivity and supercooling.

Various researchers have reported the augmentation of thermal conductivity after adding nanomaterials. Thermal properties such as phase transition temperatures, latent heat, and viscosity also vary with the addition of nanomaterials.[24] The change in latent heat is mainly due to intramolecular forces between nanomaterials and PCMs and the nanomaterials not undergoing melting during the charging process.[25] Comparatively, inorganic PCMs have more advantages than organic PCMs, such as a high energy storage density, sharp melting point, and high thermal conductivity with significant limitations of corrosiveness, supercooling, high phase-transitional volume changes, phase segregation, and incongruent melting. The encapsulation process and the addition of nanomaterials that act as nucleating agents were found to suppress the supercooling behavior in inorganic PCMs.[26] Molten salts are inorganic PCMs that are employed as heat-transfer media in high-temperature SHS systems and as PCMs in LHS systems.[27] A review article on the usage of nanoparticles with molten salts as their thermophysical property enhancers[28] provided significant insights into the various types of nanoparticles used and the way they impact the thermal and physical properties of PCMs. Solar salt (60:40 $NaNO_3$: $KNO_3$), which melts around 222−225 °C and has great thermal stability, is a typical heat-transfer fluid in solar applications.[29,30] Here, we recommend them as the energy storage media. Zhang et al.[31] synthesized nanohexagonal boron nitride-based solar salt composites and found that 0.8% boron nitride enhanced the thermal conductivity of solar salt by 16.03% and broadened the working temperature of the PCM.

Our previous studies were on the encapsulation of solar salt[32] and the addition of $Al_2O_3$ and $TiO_2$ nanoparticles with solar salt.[33] This work is an extended study on the incorporation of carbon nanotubes (CNTs) in solar salt. The aim is to enhance the thermal conductivity of solar salt (60:40 of $NaNO_3$:$KNO_3$) by adding carbon nanotubes (CNTs) at various weight concentrations of 0.1, 0.3, and 0.5% and accelerate the heat-transfer process. In addition, thermal cycling was performed to investigate the thermal reliability of the sample for the subsequent 300 cycles. Chemical compatibility and thermal characterizations, such as thermal conductivity and phase change temperatures, along with enthalpy and decomposition studies were reported for the pure and thermal cycled salts.

## 2. EXPERIMENTAL SECTION

**2.1. Selection of Materials.** In the current work, a eutectic mixture of sodium nitrate ($NaNO_3$) and potassium nitrate ($KNO_3$) in the weight ratio of 60:40, popularly recognized as solar salt, is selected as the PCM and was procured from Spectrum Chemicals, India. Carbon nanotube (CNT) was chosen as the thermal conductivity enhancer for the PCM and was procured from Sigma Aldrich. The materials were used without any additional purification.

**2.2. Preparation of the Eutectic Mixture.** A low-energy ball-milling process was utilized to synthesize the eutectic mixture of nitrate salts. A sample holder was filled with the measured quantity of the salts. Three steel balls were positioned inside the sample container. The sample holder was rotated with the principle of centrifugal force. The speed was fixed at 300 rpm for 200 min to produce the solar salt.

**2.3. Preparation of the Nano-Enhanced Solar Salt.** The solar salt prepared in Section 2.2 will be used for further preparations. A low-energy ball-milling process was employed to prepare the nano-enhanced solar salt. CNT was weighed based on the concentration, and the same was added to the solar salt in the sample holder of the ball-milling process. Then, the rotation was done for another 150 min with a speed of 300 rpm, producing the nano-enhanced solar salt. The same procedure was repeated to prepare other nano-enhanced PCM composites.

## 3. THERMAL PROPERTIES OF THE NANO-ENHANCED SOLAR SALT

Thermal properties studied in the current work and the specifications of the instruments used to study the same are listed in Table 1.

## 4. RESULTS AND DISCUSSION

**4.1. Microstructure Studies of the Composites.** Scanning electron microscopy (SEM) (VEGA 3 TESCAN) was performed to examine the morphology of the synthesized composites (Figure 1). Before the addition of carbon



https://doi.org/10.1021/acsomega.2c07571
ACS Omega 2023, 8, 17563−17572

**Table 1. Instruments and their Specifications Used to Study the Thermal Properties**

| properties | instrument and specification |
|---|---|
| morphological study | VEGA 3 TESCAN scanning electron microscope |
| | intensification of 2.5−1,000,000 X with an extreme field of view of 70.00 mm |
| | Accelerating voltage: 200−30 kV |
| thermal conductivity | LFA 467 laser flash apparatus |
| | working temperature range: −100 to 500 °C |
| | thermal diffusivity: 0.001−2000 $mm^2/s$ |
| | thermal conductivity: 0.1−4000 W/m K |
| | operated in a nitrogen atmosphere at room temperature |
| chemical compatibility | Perkin Elmer spectrum 2 infrared spectrophotometer |
| | wave number range: 500−4000 $cm^{-1}$ |
| phase change temperatures and enthalpies | DSC 6000 Perkin Elmer |
| | working temperature range: −180 to 450 °C |
| | heating and cooling rates: 0.1−100 °C/min |
| | sample is packed in an aluminum cubicle and data measured in a nitrogen atmosphere |
| thermal deterioration | TGA 4000 Perkin Elmer |
| | working temperature range: 30−1000 °C |
| | heating rate: 0.1 and 200 °C/min |
| | heating is carried out in a nitrogen atmosphere |
| thermal cycling | PCM is escalated from room temperature to a temperature above its melting point and then cooled down to room temperature. |
| | temperature was measured using a steadfast thermal cycling prearrangement consisting of a flat plate heater (1000 W) and a K-type thermocouple (±0.50 °C). |
| | sample is heated from room temperature to a temperature of 230 °C. |

nanotubes (CNTs), the solar salt appeared white at room temperature. However, after adding CNTs, the composites exhibited a dark appearance due to the presence of CNTs. The SEM image in Figure 1a shows the crystal structure of the solar salt to be nonuniform. In Figure 1b, the SEM image depicts the solar salt after adding 0.1% CNT. We can observe that the CNT adhered to the surface of the solar salt and was consistently dispersed without clustering.

**Table 2. Thermal Conductivity of Pure and Nano-Enhanced Phase Change Materials**

| | thermal conductivity (W/mK) | | augmentation (%) | |
|---|---|---|---|---|
| material | before thermal cycling | after thermal cycling | before thermal cycling | after thermal cycling |
| pure salt | 0.809 | 0.780 | | |
| salt + 0.1% CNT | 1.035 | 1.019 | 27.93 | 25.95 |
| salt + 0.3% CNT | 1.410 | 1.398 | 74.29 | 72.80 |
| salt + 0.5% CNT | 1.838 | 1.821 | 127.19 | 125.09 |

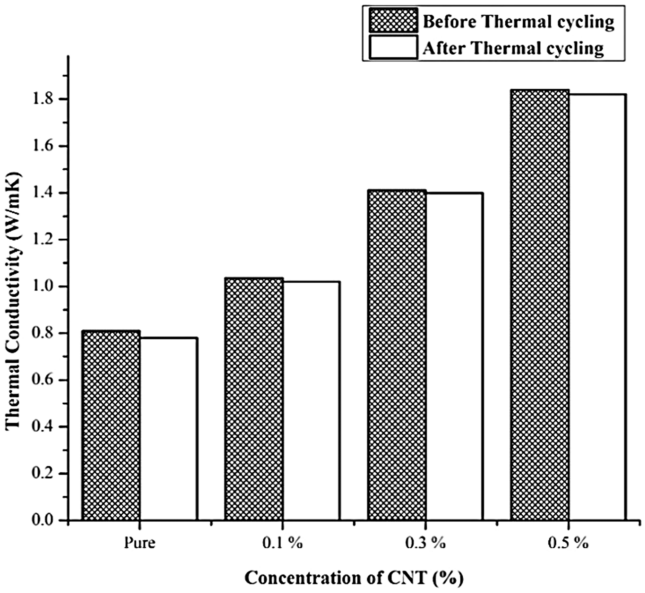


**Figure 2.** Thermal conductivity of pure and nano-enhanced phase change materials.

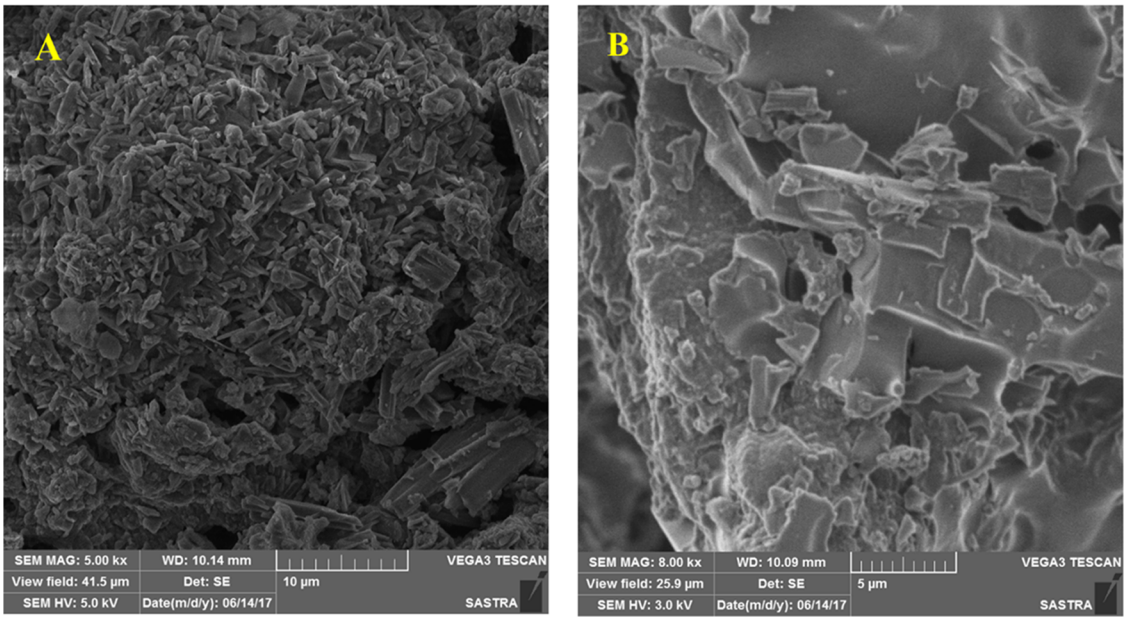


**Figure 1.** SEM images of pure (A) and CNT-enhanced solar salt (B).



https://doi.org/10.1021/acsomega.2c07571
ACS Omega 2023, 8, 17563−17572

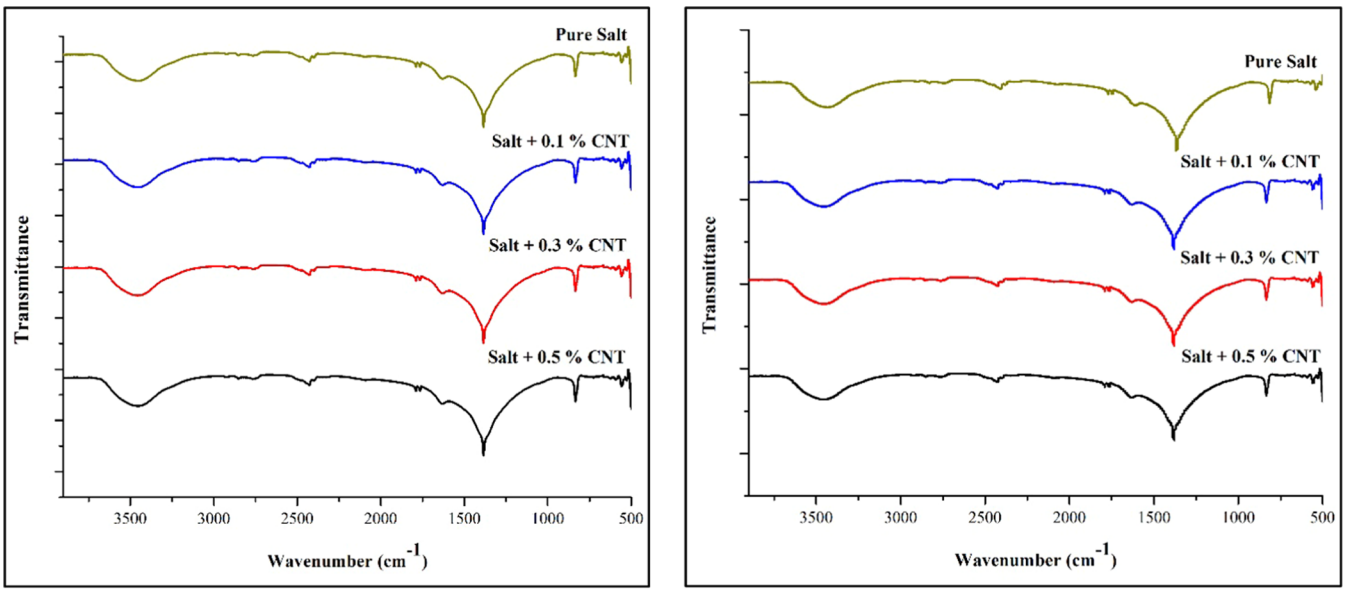


**Figure 3.** FTIR spectral peaks of pure and nano-enhanced phase change materials.

**Table 3. Phase Change Properties before Thermal Cycling**

| phase change material | melting | | solidification | | subcooling |
|---|---|---|---|---|---|
| | $T_m$ (°C) | $\Delta H_m$ (kJ/kg) | $T_s$ (°C) | $\Delta H_s$ (kJ/kg) | $T_{sc}$ (°C) |
| pure salt | 225.13 | 136.81 | 218.40 | 107.95 | 6.72 |
| salt + 0.1% CNT | 226.10 | 130.87 | 218.62 | 103.85 | 7.48 |
| salt + 0.3% CNT | 218.10 | 122.78 | 212.01 | 98.49 | 6.09 |
| salt + 0.5% CNT | 218.57 | 118.62 | 210.68 | 95.61 | 7.89 |

**4.2. Enhancement of Thermal Conductivity.** Thermal conductivity is a critical parameter in designing and fabricating a TES system to store heat. Inorganic PCMs have moderate thermal conductivity compared to organic PCMs. A low concentration of nanoparticles is added to the base PCM to enhance the thermal properties. High-conducting nanoparticles will form a thermal network with the PCM, enhancing thermal conductivity. Thermal conductivity was measured at ambient temperature in a nitrogen atmosphere using a Laser flash (LFA 467) apparatus, adapting a procedure from our previous study.[32] Table 2 and Figure 2 display the thermal conductivity of the nano-enhanced PCM with regard to thermal cycling.

It is quite apparent that the thermal conductivity was augmented linearly with the concentration of CNTs. The major reason for thermal conductivity improvement is the formation of a network structure between the CNTs and PCM[34] and CNTs moving toward the grain boundary of PCM and forming continuous quasi-2D bundles.[35] Pure salt was found to have thermal conductivities of 0.809 and 0.780 W/mK before and after thermal cycling, respectively. A significant increase was found after the addition of carbon nanotubes. Thermal conductivity was enhanced by 27.93, 74.29, and 127.19%, respectively, after adding 0.1, 0.3, and 0.5% CNTs before thermal cycling compared with pure salt.

Thermal cycling was found to have a negligible influence on thermal conductivity. After thermal cycling, the thermal conductivity enhancement was found to be 25.95, 72.80, and 125.09% in the presence of 0.1, 0.3, and 0.5% CNTs, respectively. We found that the addition of CNTs led to the formation of a network that holds the PCM and increases the thermal conductivity. From the cyclic thermal studies, we can conclude that the accumulation of nanoparticles has a lesser impact on the thermal conductivity of the solar salt after 300 cycles.

**4.3. Chemical Compatibility of Phase Change Composites.** FTIR spectral peaks were used to study the chemical composition of the phase change composites. The conventional KBr disk method was employed to measure the FTIR spectra in the frequency region ranging from 400 to 40 000 $cm^{-1}$. Figure 3a,b depicts the FTIR spectral peaks of the samples before and after thermal cycling, respectively. It can be clearly seen that all of the curves are quite similar in the spectral region. The characteristic peaks at 2432.41 and 1386.92 $cm^{-1}$ indicate the presence of nitrate in $KNO_3$. For all composites, a peak is found at 3467.03 $cm^{-1}$, which is attributed to the hydroxyl (O-H) stretching, and another bending of $\delta$-OH at 1785.86 and 1735.17 $cm^{-1}$, suggesting the evaporation of water from the sample. The broad peak 3 formed at 1386.92 $cm^{-1}$ indicates the $\nu\bar{3}NO\bar{3}$ stretch. The peak formed at 847.75 $cm^{-1}$ is strong and shows the presence of sodium nitrate crystals. From the FTIR spectra of pure and encapsulated samples upon cycling, it is evident that the frequency remained quite identical in both the functional group and fingerprint regions. The results confirm that only physical interaction took place between the salt and CNTs, with an absence of any chemical reaction.

**4.4. Phase Conversion Properties of Phase Change Composites.** Differential scanning calorimetric analysis was performed to determine the phase-transition temperatures and their corresponding enthalpies. The samples were heated from ambient temperature to a temperature above their melting point and then chilled to room temperature at set heating and cooling rates. Three cycles of heating and cooling were performed, and the average was taken as the actual reading. The quantity of heat absorbed or released was measured for the sample with respect to a reference sample, and latent heat


https://doi.org/10.1021/acsomega.2c07571
ACS Omega 2023, 8, 17563−17572

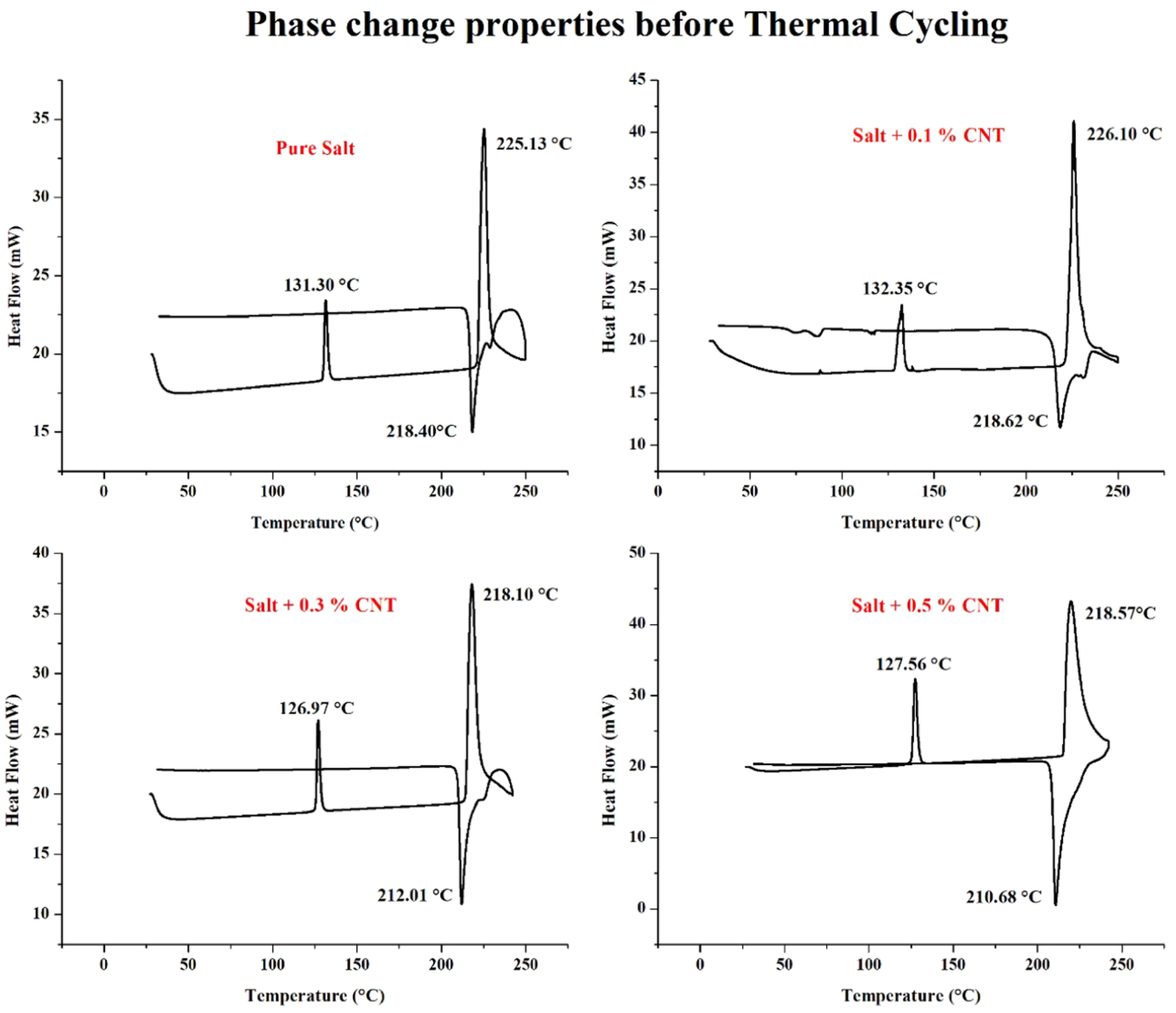


**Figure 4.** DSC Thermograms of the pure and nano-enhanced phase change materials before thermal cycling.

**Table 4. Phase Change Properties after Thermal cycling**

| phase change material | melting | | solidification | | subcooling |
|---|---|---|---|---|---|
| | $T_m$ (°C) | $\Delta H_m$ (kJ/kg) | $T_s$ (°C) | $\Delta H_s$ (kJ/kg) | $T_{sc}$ (°C) |
| pure salt | 224.53 | 131.52 | 219.83 | 106.75 | 4.70 |
| salt + 0.1% CNT | 226.47 | 128.11 | 220.20 | 101.85 | 6.27 |
| salt + 0.3% CNT | 228.84 | 120.56 | 222.08 | 96.75 | 6.76 |
| salt + 0.5% CNT | 228.83 | 116.75 | 219.35 | 91.98 | 9.48 |

was calculated by integrating the onset and offset peaks during the phase transition.

Two peaks were observed for the pure and nano-enhanced salts. A minor peak in the temperature range of 110−120 °C is correlated to the solid−solid conversion. A major peak in the temperature range of 215−230 °C is correlated to the actual solid−liquid phase change from which the phase change temperatures and their latent heat values are calculated. Table 3 presents the phase-transition properties of the PCM before thermal cycling. Figure 4 depicts the DSC thermograms of the samples before thermal cycling. Samples were packed in an aluminum crucible and heated from room temperature to a set temperature of 250 °C. The heating and cooling rates were fixed at 10 °C/min. Pure solar salt was found to thaw and freeze at 225.13 and 218.40 °C with a subcooling of 6.72 °C. The latent heat values were calculated to be 136.81 and 107.95 kJ/kg for the melting and solidification processes, correspondingly.

The presence of nanoparticles caused a minor decline in the thermal properties of the PCM. Increasing or stabilizing the latent heat after the addition of nanoparticles is highly difficult. After adding CNTs to PCM, heterogeneous nucleation is induced, leading to an increase in nucleation points, thereby reducing the grain size of the PCM. The melting process is associated with the destruction of the molecular assembly. As a result of the addition of CNTs, the crystallization process creates an orderly arrangement of the molecules of PCM, which may require more heat energy to break them, leading to an increase in the melting temperature. In contrast, the melting temperature decreases with a reduction in the grain size during the crystallization process.[36]



https://doi.org/10.1021/acsomega.2c07571
ACS Omega 2023, 8, 17563−17572

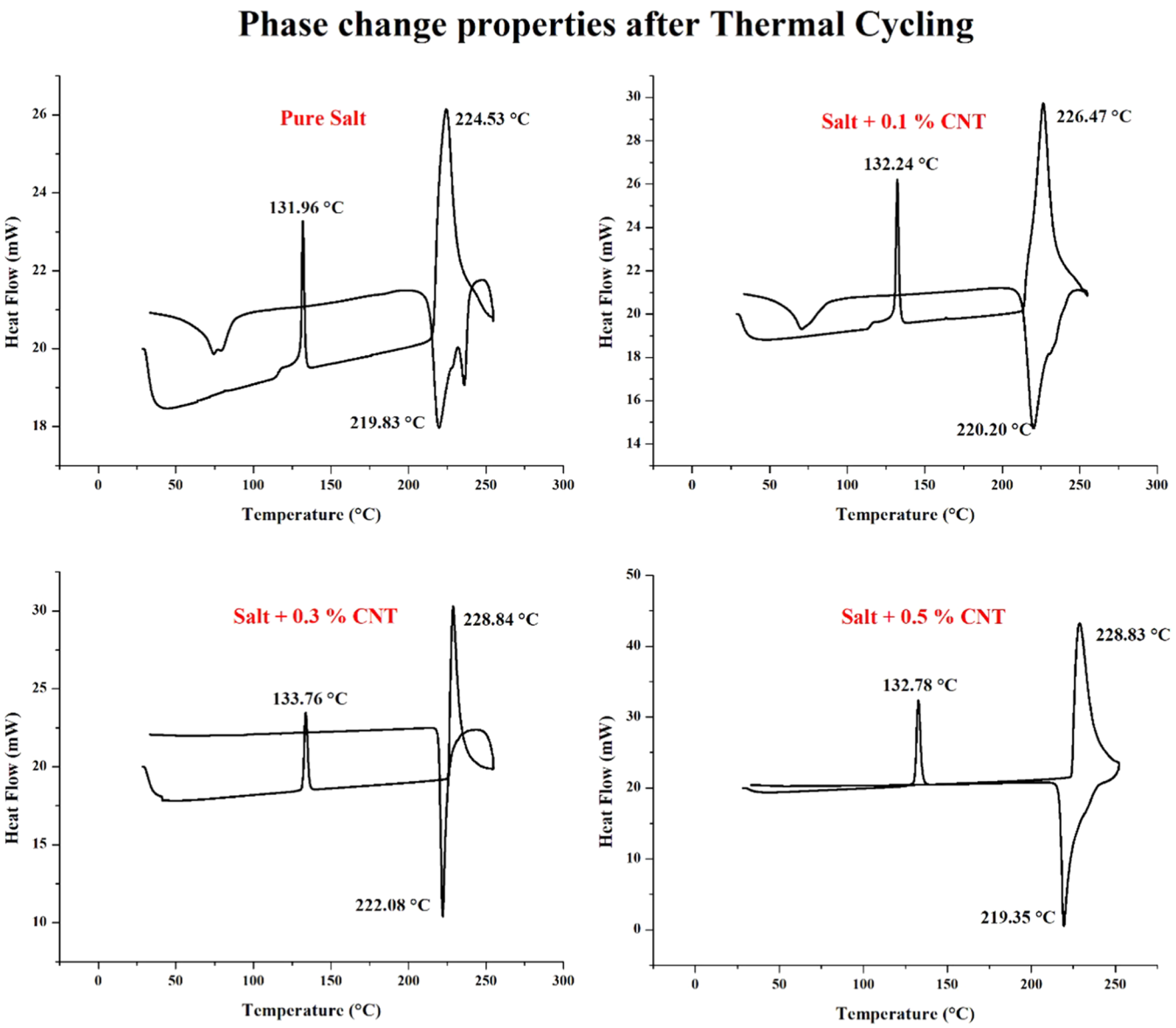


**Figure 5.** DSC thermograms of the pure and nano-enhanced phase change materials after thermal cycling.

**Table 5. Percentage Change in Thermal Properties after Thermal Cycling**

| | melting (%) | | solidification (%) | |
|---|---|---|---|---|
| phase change material | $T_m$ | $\Delta H_m$ | $T_s$ | $\Delta H_s$ |
| pure salt | 0.26 | 3.87 | 0.65 | 1.11 |
| salt + 0.1% CNT | 0.59 | 6.36 | 0.82 | 3.80 |
| salt + 0.3% CNT | 1.65 | 11.88 | 1.68 | 10.38 |
| salt + 0.5% CNT | 1.64 | 14.67 | 0.43 | 14.80 |

After adding nanoparticles, the composite PCM was found to liquefy and harden at 226.10 and 218.40 °C, respectively, in the presence of 0.1% CNT, with the corresponding latent heat values being 130.87 and 103.85 kJ/kg, respectively. The change in latent heat after the addition of CNTs is due to the salts undergoing a phase change process after absorbing heat. CNTs did not undergo any phase change during the process, thus limiting their overall latent heat. Therefore, we can understand that the latent heat is mainly dependent on the PCM and not on the addition of nanomaterials. The melting temperature decreases with an increase in CNT concentration. The melting and solidification temperatures were found to be 218.10, 212.01 °C and 218.57, 210.68 °C with 0.3% and 0.5% CNTs, respectively. The latent heat also decreased with an increase in CNT concentration. The latent heat values were found to be 122.78, 98.49, and 118.62, 95.61 kJ/kg during melting and solidification with the addition of 0.3 and 0.5% CNTs, respectively. The accumulation of CNTs has enhanced the thermal conductivity of the base salt and slightly decreased the latent heat storage capacity.

Thermal cycling was found to have a momentous influence on the thermal properties of salt. Table 4 presents the phase change properties of the composites after thermal cycling, and Figure 5 depicts the DSC thermograms of the composites after thermal cycling. After 300 thermal cycles, pure salt was found to thaw and freeze at 224.53 and 219.83 °C, with their latent heat values being 131.52 and 106.75 kJ/kg, respectively. After cycling, the melting temperature of composites increased compared to that of pure salt. The latent heat decreased compared to that of the composites before thermal cycling.



https://doi.org/10.1021/acsomega.2c07571
ACS Omega 2023, 8, 17563−17572

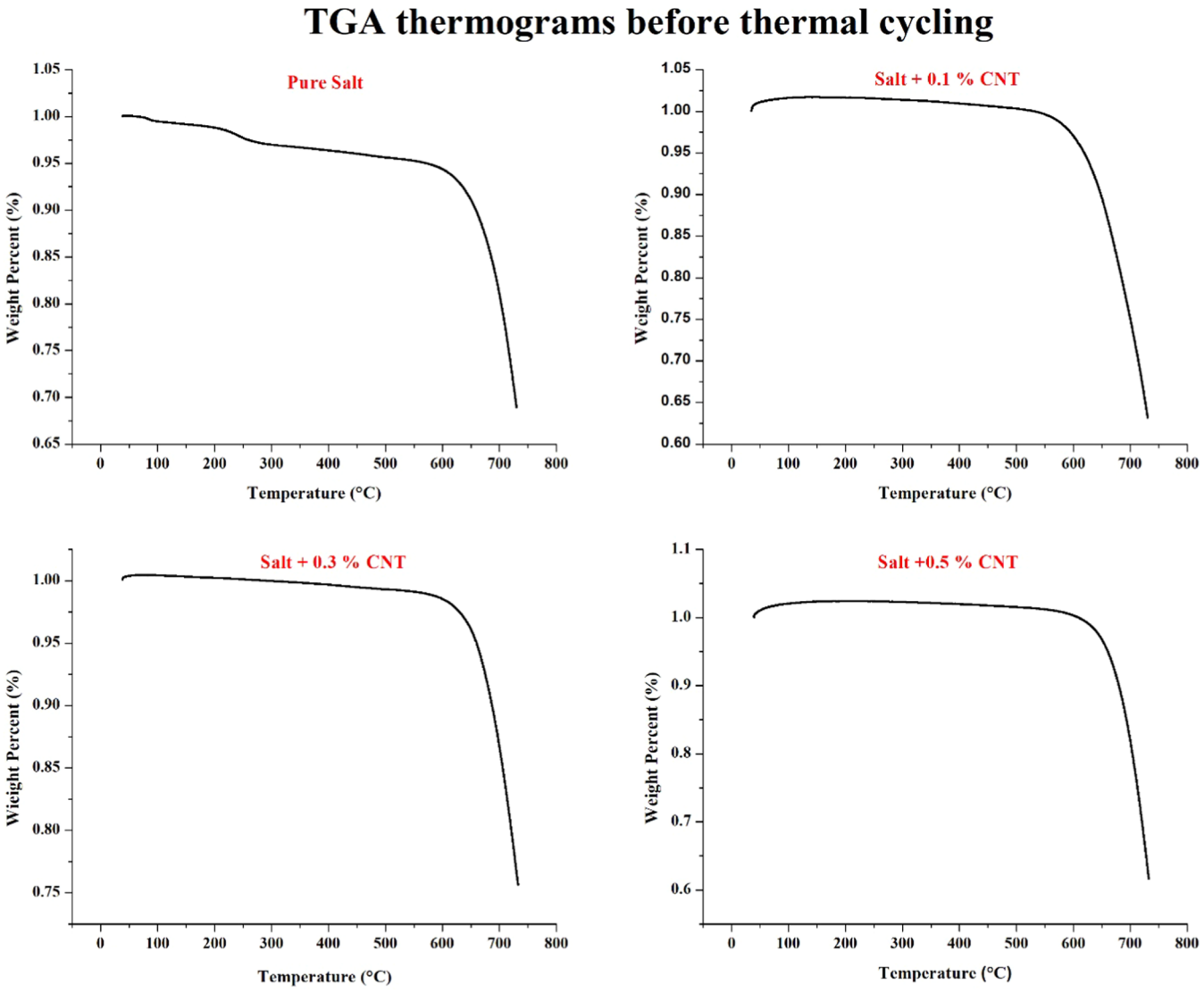


**Figure 6.** TGA thermograms of the composites before thermal cycling.

With 0.1% CNT, the salt melted and solidified at 226.47 and 220.20 °C and possessed latent heat values of 128.11 and 101.85 kJ/kg, respectively. The melting temperature further increased with an upsurge in the CNT concentration. Melting and solidification temperatures were found to be 228.84, 222.08 °C, and 228.83, 219.35 °C with 0.3 and 0.5% CNTs, respectively. The latent heat values were found to be 120.56, 96.75, and 116.75, 91.95 kJ/kg during melting and solidification for 0.3 and 0.5% of CNTs, respectively. The percentage change in the thermal properties of the nano-enhanced PCM compared to the pure salt is presented in Table 5. After thermal cycling, we can find a minor change in the thermal properties of composites.

The melting and solidification temperatures were found to vary from 0.20 to 1.70%, which is a minor change in large-scale applications. The latent heat was found to decrease with an increase in CNT concentration. In the presence of 0.5% CNTs, the latent heat was reduced by 14.67 and 14.80% during melting and solidification, correspondingly, compared to that of pure solar salt.

**4.5. Subcooling Degree.** Subcooling temperature denotes the temperature variance between the melting and solidification points. The subcooling temperature must be minimal for thermal energy storage applications. Solar salt was found to have subcooling temperatures of 6.72 and 4.70 °C before and after thermal cycling, respectively. This subcooling temperature has a direct influence on the crystallization rate of the PCM. The subcooling temperatures were found to be 7.48, 6.09, and 7.89 °C in the presence of 0.1, 0.3, and 0.5% CNTs, respectively. After thermal cycling, the subcooling temperatures were found to be 6.27, 6.76, and 9.48 °C after adding 0.1, 0.3, and 0.5% CNTs, respectively. The change in the subcooling temperature was minimal on applying these composites in a thermal energy storage system.

**4.6. Thermal Steadiness of Phase Change Composites.** The thermal steadiness of a PCM is a vital parameter to determine the temperature range that can be employed without affecting its weight change. Thermogravimetric analysis is the method used to study the thermal degradation of the sample with reference to increased temperature. The samples are loaded in a capsule and heated from ambient conditions to a set temperature of 750 °C with a heating rate of 10 °C/min, and the weight loss is calculated with respect to the increase in temperature.



https://doi.org/10.1021/acsomega.2c07571
ACS Omega 2023, 8, 17563−17572

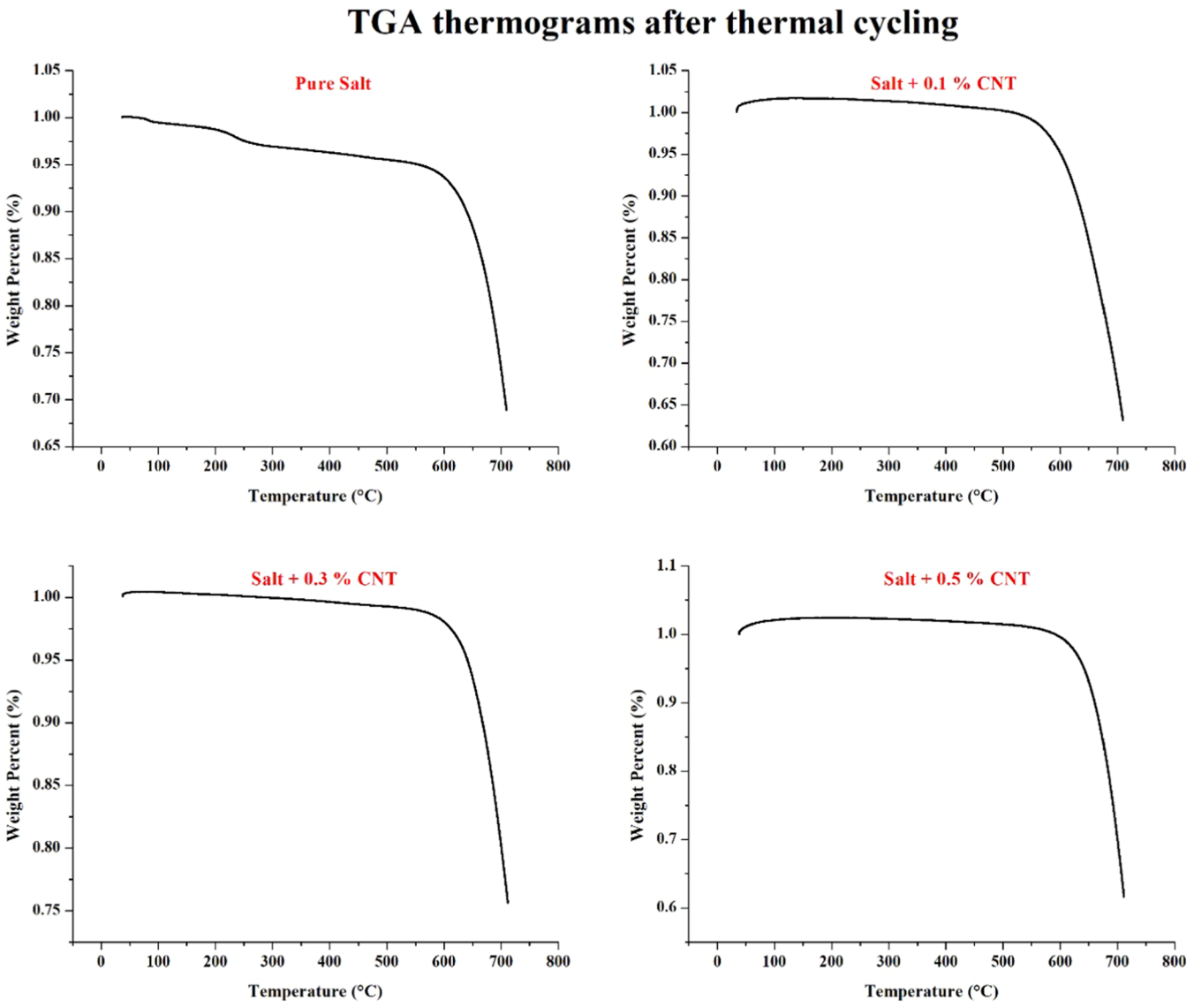


**Figure 7.** TGA thermograms of the composites after thermal cycling.

**Table 6. Summary of TGA Data**

| | before thermal cycling | | after thermal cycling | |
|---|---|---|---|---|
| phase change material | $T_{wi}$ (°C) | $T_{max}$ (°C) | $T_{wi}$ (°C) | $T_{max}$ (°C) |
| pure salt | 594.21 | 719.75 | 578.38 | 701.34 |
| salt + 0.1% CNT | 544.15 | 724.16 | 526.48 | 700.60 |
| salt + 0.3% CNT | 588.32 | 722.69 | 572.87 | 704.28 |
| salt + 0.5% CNT | 592.74 | 727.11 | 580.59 | 710.18 |

Figure 6 displays the TGA thermograms of composites before thermal cycling. All of the composites were found to have a single weight loss with respect to temperature. The weight loss was minimal till a temperature of 590 °C for pure salt, and the maximum weight loss was found at 720 °C. After the addition of CNTs, the temperature of weight loss initiation and the maximum weight loss changed significantly compared to that of pure salt. Afterward, the weight loss of 0.1% CNTs originated at 544 °C, which was much lower than that of pure salt and showed maximum weight loss until 725 °C. As the CNT concentration increases, the initiation temperature and maximum weight loss temperature did not change much compared to that of pure salt. In the presence of 0.3% CNTs, the weight loss began at 588 °C, and the maximum weight loss was seen at a temperature of 722 °C. After adding 0.5% CNTs, the weight loss was initiated at 592 °C, and the maximum weight loss was observed at a temperature of 727 °C.

TGA analysis of pure composites indicated that they could be utilized in systems with a maximum working temperature of 600 °C, beyond which the composites will exhibit weight loss, which can lead to a lowering of the energy storage density of the PCM on a larger scale. Figure 7 displays TGA thermograms of the composites after thermal cycling. Compared to the composites before thermal cycling, the weight loss of the composites after thermal cycling also followed the same trend. All composites exhibited a single weight loss curve.

After thermal cycling, pure salt exhibited a weight loss at 578 °C and the maximum weight loss at 701 °C. A deviation of 20 °C was found in the temperatures related to pure salt before thermal cycling. The addition of CNTs was found to have the same impact on the PCM, similar to that before thermal cycling. After adding 0.1% CNTs, weight loss initiated at 526 °C and was severe until 700 °C. The temperatures increased with an increase in the concentration of CNTs. In the presence


https://doi.org/10.1021/acsomega.2c07571
ACS Omega 2023, 8, 17563−17572

of 0.3% CNTs, weight loss commenced at 572 °C and maximum weight loss occurred at 704 °C. After adding 0.5% CNTs, the composites exhibited a weight loss at 580 °C with the maximum weight loss at 710 °C. We can infer from the thermal analysis that the composites could withstand 300 thermal cycles without any change in thermal degradation behaviors, which is a highly promising aspect for their application in high-temperature energy storage applications for enhanced heat transfer. Table 6 summarizes the TGA data of composites before and after thermal cycling. $T_{wi}$ and $T_{max}$ indicate the temperature of weight loss initiation and temperature of maximum weight loss, respectively.

## 5. CONCLUSIONS AND FUTURE STUDIES

Solar salt has been utilized as a direct heat-transfer fluid in high-temperature solar-based applications. We propose solar salt as a phase change material for high-temperature applications due to its high energy storage capacity. To improve its thermal conductivity, varied carbon nanotube (CNT) concentrations were added to the salt using the ball-milling method. Thermal properties of composites were studied before and after 300 thermal cycles. The thermal conductivity, phase change properties, and thermal steadiness were studied using an LFA 467 analyzer, a DSC 6000 Perkin Elmer analyzer, and a TGA 4000 Perkin Elmer analyzer, respectively, and the significant findings are listed below,

- Pure salt possesses thermal conductivities of 0.809 and 0.780 W/mK before and after thermal cycling. The enhancements in thermal conductivity were found to be 27.93, 74.29, and 127.19% with the addition of 0.1, 0.3, and 0.5% CNTs, respectively. After thermal cycling, the enhancements were 25.95, 72.80, and 125.09% compared to that of pure salt.
- Pure salt liquefied and hardened at 225.13 and 218.40 °C. After thermal cycling, the same were 224.53 and 219.83 °C, respectively. Latent heat values were found to be 136.81 and 107.95 kJ/kg before thermal cycling, and they reduced by 3.87 and 1.11% after thermal cycling.
- Minor changes in phase change properties were found after the addition of CNTs. In the presence of 0.5% CNTs, the composite was found to thaw and freeze at 218.57 and 95.61 °C, correspondingly. Enthalpies were reduced by 14.67 and 14.80% before and after thermal cycling compared to those of pure salt.
- The presence of CNTs increased the thermal stability of the composites. The composites were thermally stable until a temperature of 600 °C, after which there was a rapid weight loss. In pure salt, weight loss initiated at 594.21 °C, and after thermal cycling, it was 578.38 °C. After adding 0.5% CNTs, weight loss was initiated at 592.74 °C and was rapid till 580.59 °C.

Thermal characterization of solar salt and CNT-based solar salt composites revealed that the composites could be involved in superior heat transfer in high-temperature solar-based energy storage systems. Furthermore, the problem of the salts having low conductivity was overcome to some extent by the accumulation of nanomaterials. This has further led to additional research on the lowering of latent heat. Subsequent studies can be conducted with the addition of a wider range of nanomaterials to solar salt, along with the study of the mechanism of lowering of the latent heat in the presence of nanomaterials.

## AUTHOR INFORMATION


### Corresponding Author

**Saboor Shaik** − *Department of Thermal and Energy Engineering, School of Mechanical Engineering (SMEC), Vellore Institute of Technology, Vellore 632014 Tamil Nadu, India;* orcid.org/0000-0002-0490-4766; Email: saboor.nitk@gmail.com

### Authors

**Pethurajan Vigneshwaran** − *Department of Thermal and Energy Engineering, School of Mechanical Engineering (SMEC), Vellore Institute of Technology, Vellore 632014 Tamil Nadu, India; Nanotechnology Research Laboratory, Department of Mechanical Engineering, National Institute of Technology (NIT), Tiruchirappalli 620015 Tamil Nadu, India*

**Sivan Suresh** − *Nanotechnology Research Laboratory, Department of Mechanical Engineering, National Institute of Technology (NIT), Tiruchirappalli 620015 Tamil Nadu, India;* orcid.org/0000-0002-2261-2687

**Mohamed Abbas** − *Electrical Engineering Department, College of Engineering, King Khalid University, Abha 61421, Saudi Arabia; Electronics and Communications Department, College of Engineering, Delta University for Science and Technology, Gamasa 35712, Egypt*

**Chanduveetil Ahamed Saleel** − *Department of Mechanical Engineering, College of Engineering, King Khalid University, Abha 61421, Saudi Arabia*

**Erdem Cuce** − *Low/Zero Carbon Energy Technologies Laboratory, Faculty of Engineering and Architecture and Department of Mechanical Engineering, Faculty of Engineering and Architecture, Recep Tayyip Erdogon University, Zihni Derin Campus, Rize 53100, Turkey*

Complete contact information is available at: https://pubs.acs.org/10.1021/acsomega.2c07571


### Notes

The authors declare no competing financial interest.

All authors have realized and accepted the data of the submitted manuscript. The paper presents unique work not earlier published in a similar form and not presently under consideration by another journal. The authors followed ethical guidelines.

The authors declare that they have no known competing financial interests or personal relationships that could have influenced the work reported in this paper.

## ACKNOWLEDGMENTS

The authors extend their appreciation to the Deanship of Scientific Research at King Khalid University for funding this work through the Large Group Research Project under grant number RGP2/45/44

## REFERENCES

(1) Yang, J.; Tang, L.-S.; Bai, L.; Bao, R.-Y.; Liu, Z.-Y.; Xie, B.-H.; Yang, M.-B.; Yang, W. High-performance composite phase change materials for energy conversion based on macroscopically three-dimensional structural materials. *Mater. Horiz.* **2019**, *6*, 250−273.

(2) Ibrahim, N. I.; Al-Sulaiman, F. A.; Rahman, S.; Yilbas, B. S.; Sahin, A. Z. Heat transfer enhancement of phase change materials for thermal energy storage applications: A critical review. *Renewable Sustainable Energy Rev.* **2017**, *74*, 26−50.



https://doi.org/10.1021/acsomega.2c07571
*ACS Omega* 2023, 8, 17563−17572

(3) Wei, G.; Wang, G.; Xu, C.; Ju, X.; Xing, L.; Du, X.; Yang, Y. Selection principles and thermophysical properties of high temperature phase change materials for thermal energy storage: A review. *Renewable Sustainable Energy Rev.* **2018**, *81*, 1771−1786.
(4) Kalnæs, S. E.; Jelle, B. P. Phase change materials and products for building applications: A state-of-the-art review and future research opportunities. *Energy Buildings* **2015**, *94*, 150−176.
(5) Fadl, M.; Eames, P. C. An experimental investigation of the heat transfer and energy storage characteristics of a compact latent heat thermal energy storage system for domestic hot water applications. *Energy* **2019**, *188*, No. 116083.
(6) Yuan, F.; Li, M.-J.; Ma, Z.; Jin, B.; Liu, Z. Experimental study on thermal performance of high-temperature molten salt cascaded latent heat thermal energy storage system. *Int. J. Heat Mass Transfer* **2018**, *118*, 997−1011.
(7) Soni, V.; Kumar, A.; Jain, V. K. Performance evaluation of nano-enhanced phase change materials during discharge stage in waste heat recovery. *Renewable Energy* **2018**, *127*, 587−601.
(8) Tao, Y. B.; He, Y.-L. A review of phase change material and performance enhancement method for latent heat storage system. *Renewable Sustainable Energy Rev.* **2018**, *93*, 245−259.
(9) Liu, H.; Wang, X.; Wu, D. Innovative design of micro-encapsulated phase change materials for thermal energy storage and versatile applications: a review. *Sustainable Energy Fuels* **2019**, *3*, 1091−1149.
(10) Gulfam, R.; Zhang, P.; Meng, Z. Advanced thermal systems driven by paraffin-based phase change materials−A review. *Appl. Energy* **2019**, *238*, 582−611.
(11) Jamekhorshid, A.; Sadrameli, S. M.; Farid, M. A review of microencapsulation methods of phase change materials (PCMs) as a thermal energy storage (TES) medium. *Renewable Sustainable Energy Rev.* **2014**, *31*, 531−542.
(12) Rostami, S.; Afrand, M.; Shahsavar, A.; Sheikholeslami, M.; Kalbasi, R.; Aghakhani, S.; Shadloo, M. S.; Oztop, H. F. A review of melting and freezing processes of PCM/nano-PCM and their application in energy storage. *Energy* **2020**, *211*, No. 118698.
(13) Wang, J.; Xie, H.; Xin, Z. Thermal properties of paraffin based composites containing multi-walled carbon nanotubes. *Thermochim. Acta* **2009**, *488*, 39−42.
(14) Dheep, G. R.; Sreekumar, A. Influence of nanomaterials on properties of latent heat solar thermal energy storage materials−A review. *Energy Convers. Manage.* **2014**, *83*, 133−148.
(15) Zhang, H.; Rindt, C. C. M.; Smeulders, D. M. J.; Nedea, S. V. Nanoscale heat transfer in carbon nanotubes-sugar alcohol composite as heat storage materials. *J. Phys. Chem. C* **2016**, *120*, 21915−21924.
(16) Hayat, M. A.; Chen, Y.; Bevilacqua, M.; Li, L.; Yang, Y. Characteristics and potential applications of nano-enhanced phase change materials: A critical review on recent developments. *Sustainable Energy Technol. Assess.* **2022**, *50*, No. 101799.
(17) Cao, R.; Chen, S.; Wang, Y.; Han, N.; Liu, H.; Zhang, X. Functionalized carbon nanotubes as phase change materials with enhanced thermal, electrical conductivity, light-to-thermal, and electro-to-thermal performances. *Carbon* **2019**, *149*, 263−272.
(18) Wang, J.; Xie, H.; Xin, Z.; Li, Y.; Chen, L. Enhancing thermal conductivity of palmitic acid based phase change materials with carbon nanotubes as fillers. *Sol. Energy* **2010**, *84*, 339−344.
(19) Wu, X.; Wang, C.; Wang, Y.; Zhu, Y. Experimental study of thermo-physical properties and application of paraffin-carbon nanotubes composite phase change materials. *Int. J. Heat Mass Transfer* **2019**, *140*, 671−677.
(20) Zou, D.; Ma, X.; Liu, X.; Zheng, P.; Hu, Y. Thermal performance enhancement of composite phase change materials (PCM) using graphene and carbon nanotubes as additives for the potential application in lithium-ion power battery. *Int. J. Heat Mass Transfer* **2018**, *120*, 33−41.
(21) Wang, C.; Chen, K.; Huang, J.; Cai, Z.; Hu, Z.; Wang, T. Thermal behavior of polyethylene glycol based phase change materials for thermal energy storage with multiwall carbon nanotubes additives. *Energy* **2019**, *180*, 873−880.
(22) Zhang, N.; Yuan, Y.; Yuan, Y.; Cao, X.; Yang, X. Effect of carbon nanotubes on the thermal behavior of palmitic−stearic acid eutectic mixtures as phase change materials for energy storage. *Sol. Energy* **2014**, *110*, 64−70.
(23) Shen, S.; Tan, S.; Wu, S.; Guo, C.; Liang, J.; Yang, Q.; Xu, G.; Deng, J. The effects of modified carbon nanotubes on the thermal properties of erythritol as phase change materials. *Energy Convers. Manage.* **2018**, *157*, 41−48.
(24) Amudhalapalli, G. K.; Devanuri, J. K. Synthesis, characterization, thermophysical properties, stability and applications of nanoparticle enhanced phase change materials−A comprehensive review. *Therm. Sci. Eng. Prog.* **2021**, No. 101049.
(25) Liu, X.; Rao, Z. Experimental study on the thermal performance of graphene and exfoliated graphite sheet for thermal energy storage phase change material. *Thermochim. Acta* **2017**, *647*, 15−21.
(26) Junaid, M. F.; Rehman, Z.u.; Čekon, M.; Čurpek, J.; Farooq, R.; Cui, H.; Khan, I. Inorganic phase change materials in thermal energy storage: A review on perspectives and technological advances in building applications. *Energy Buildings* **2021**, *252*, No. 111443.
(27) Kenisarin, M. M. High-temperature phase change materials for thermal energy storage. *Renewable Sustainable Energy Rev.* **2010**, *14*, 955−970.
(28) Aljaerani, H. A.; Ahmad, M.; Samykano, R.; Saidur, A. K.; Pandey; Kadirgama, K. Nanoparticles as molten salts thermophysical properties enhancer for concentrated solar power: A critical review. *J. Energy Storage* **2021**, *44*, No. 103280.
(29) Grena, R.; Tarquini, P. Solar linear Fresnel collector using molten nitrates as heat transfer fluid. *Energy* **2011**, *36*, 1048−1056.
(30) Liu, M.; Saman, W.; Bruno, F. Review on storage materials and thermal performance enhancement techniques for high temperature phase change thermal storage systems. *Renewable Sustainable Energy Rev.* **2012**, *16*, 2118−2132.
(31) Zhang, Y.; Wang, M.; Li, J.; Wang, H.; Zhao, Y. Improving thermal energy storage and transfer performance in solar energy storage: Nanocomposite synthesized by dispersing nano boron nitride in solar salt. *Sol. Energy Mater. Sol. Cells* **2021**, *232*, No. 111378.
(32) Pethurajan, V.; Suresh, S.; Mojiri, A.; Konatt, A. J. Microencapsulation of nitrate salt for solar thermal energy storage-synthesis, characterisation and heat transfer study. *Sol. Energy Mater. Sol. Cells* **2020**, *206*, No. 110308.
(33) Jeyaseelan, T. R.; Azhagesan, R. N.; Pethurajan, V. Thermal characterization of $NaNO_3/KNO_3$ with different concentrations of $Al_2O_3$ and $TiO_2$ nanoparticles. *J. Therm. Anal. Calorim.* **2019**, *136*, 235−242.
(34) Harish, S.; Ishikawa, K.; Chiashi, S.; Shiomi, J.; Maruyama, S. Anomalous thermal conduction characteristics of phase change composites with single-walled carbon nanotube inclusions. *J. Phys. Chem. C* **2013**, *117*, 15409−15413.
(35) Volkov, A. N.; Zhigilei, L. V. Scaling laws and mesoscopic modeling of thermal conductivity in carbon nanotube materials. *Phys. Rev. Lett.* **2010**, *104*, No. 215902.
(36) Yu, Q.; Zhang, C.; Lu, Y.; Kong, Q.; Wei, H.; Yang, Y.; Gao, Q.; Wu, Y.; Sciacovelli, A. Comprehensive performance of composite phase change materials based on eutectic chloride with SiO2 nanoparticles and expanded graphite for thermal energy storage system. *Renewable Energy* **2021**, *172*, 1120−1132.


https://doi.org/10.1021/acsomega.2c07571
*ACS Omega* 2023, 8, 17563−17572